**PFG 2013 / 3, 0139–0148**
Stuttgart, June 2013

**Article**

# Habitat Mapping from Optical and SAR Satellite Data: Implications of Synergy and Uncertainty for Landscape Analysis

Stefan Erasmi, Göttingen

**Keywords:** habitat mapping, SAR data, RapidEye, accuracy assessment, landscape metrics

**Summary:** Satellite based habitat maps are the main source for the analysis of landscape pattern and its effect on species diversity and ecosystem functions. Nonetheless, only few studies systematically investigated the optimal constellation of multi-source satellite input data for habitat mapping and the effect of mapping accuracy on landscape pattern indices and hence on ecological analysis. The present study underlines the importance of a careful selection of input data for land cover type classification and highlights the synergistic potential of optical/SAR data fusion for habitat mapping purposes. With regard to landscape analysis the study reveals the impact of classification accuracy on variation in landscape metrics. This impact is not uniform and not always directly related to classification accuracy but is depending on the nature of landscape metrics. Area metrics show strong variations with the magnitude of variation being much higher than the classification errors whereas variation of diversity and connectivity measures is significantly below the classification error. Finally, it is demonstrated that spatial uncertainty in land cover maps has to be addressed in any landscape analysis at spatial scale.

**Zusammenfassung:** *Die Habitatkartierung aus Daten optischer und SAR-Satelliten: Synergieeffekte und Unsicherheiten bei der Analyse der Landschaft.* Die Analyse der Zusammenhänge zwischen Landschaftsmustern und Artenvielfalt bzw. Ökosystemfunktionen im Allgemeinen ist in vielen Fällen auf satellitenbasierte Habitatkartierungen gestützt. Hierbei wird aber nur in wenigen Fällen untersucht, welche Sensoren und Aufnahmezeitpunkte am besten geeignet sind. Darüber hinaus wird in den meisten Fällen nicht berücksichtigt, welche Auswirkungen die Klassifikationsgenauigkeit auf die Berechnung von Landschaftsmaßen und damit auf die Auswertung ökologischer Zusammenhänge haben kann. In diesem Zusammenhang hebt der vorliegende Beitrag die Wichtigkeit und Notwendigkeit der sorgsamen Auswahl von Satellitendaten für Landbedeckungskartierungen hervor und unterstreicht das Potential der Fusion von optischen und SAR-Daten für qualitative Fernerkundungsauswertungen. Die Ergebnisse machen den Einfluss der Klassifikationsgenauigkeit auf die Berechnung von Landschaftsmaßen (landscape metrics) deutlich. Dieser Einfluss ist nicht einheitlich sondern von den Eigenschaften der Maße abhängig, wobei flächenbezogene Indikatoren einer stärkeren Schwankung unterworfen sind als Konnektivitäts- und Diversitätsmaße. Insgesamt unterstreichen die Ergebnisse die Notwendigkeit der Berücksichtigung von Unsicherheiten in den Datengrundlagen bei der räumlich expliziten Landschaftsanalyse.

## 1 Introduction

Human-dominated landscapes are characterised by complex mosaics of agricultural, semi-natural and natural habitats. Several studies have shown that landscape heterogeneity affects species diversity and ecosystem functions, such as pollination (e.g. Westphal et al. 2006, Tscharntke et al. 2012). Landscape complexity in this context is routinely quantified by measures of landscape composition and configuration (landscape metrics). Remote sensing based land cover and habitat


www.schweizerbart.de
DOI: 10.1127/1432-8364/2013/0165
1432-8364/13/0165 $ 2.50

maps provide the base for the calculation of those landscape metrics and have been widely used for ecological studies that account for spatial scale as an indicator for ecological diversity (e.g. GILLESPIE et al. 2008, PEROVIC et al. 2010). The statistical background and behaviour of landscape metrics is well documented (RIITTERS et al. 1995, NEEL et al. 2004). Less attention has been paid to the spatial uncertainty of the satellite maps underlying the landscape metrics calculation. Uncertainty in this context can be a function of the classification scheme, the spatial/thematic scale and the classification accuracy and has been subject to investigation in many theoretical studies based on synthetic data (e.g. BUYANTUYEV & WU 2007, LANGFORD et al. 2006, WICKHAM et al. 1997, SAURA 2002). However, in a recent study LECHNER et al. (2012) reported that only 1 out of 59 studies in landscape ecology accounted for the effect of classification accuracy on landscape metrics and hence on ecological analyses.

In this study, a multi-sensor optical and SAR satellite dataset (RapidEye, RADARSAT-2, TerraSAR-X) is evaluated for its ability to map land cover type with a focus on functional habitat types (semi-natural habitats) for ecological studies. The quality of land cover maps is documented in terms of classification accuracy and variation in accuracy measures. The synergy of optical and SAR data for mapping land cover is evaluated by means of classification accuracy and relative importance of input variables. In a second step, the effect of classification accuracy on variations in landscape metrics is tested. Here, the author follows the hypothesis of LANGFORD et al. (2006) and LECHNER et al. (2012) that uncertainty in land cover maps induces errors in landscape pattern analyses.

## 2 Data

The study area is located in the vicinity of the UNESCO-biosphere reserve "Schorfheide-Chorin" in eastern Germany, about 50 kilometres north of Berlin. It is characterized by sander areas and moraines which are representative for the glacially formed lowlands of north-eastern Germany. The cultural landscape is dominated by intensive agricultural production fields (cropland and grassland) that are flanked by many small to large lakes, fens and mires. Besides intensive agriculture, there are considerable areas of extensive cultivation and semi-natural habitats.

### 2.1 *Field Data*

Land use type was mapped in a field campaign in 2009 in 5 different land use clusters comprising more than 3000 polygons and covering a total area of 22,891 ha. Additionally, information on crop type and productive grassland were available for the investigation period (2011) from the agricultural ministry of the federal state of Brandenburg. These two data sources were merged to a comprehensive ground truth dataset for our investigation. In total, the land cover is represented by a two-level classification system including 6 general land use types at the first level and 18 habitat subtypes at the second level. However, earlier investigations (ERASMI et al. in press) have shown that some of the thematic classes at the sub-level are not well represented by the available satellite data. Furthermore, not all of the subtypes are relevant for habitat and biodiversity mapping within the present case study. This is why in this study the number of subtypes was aggregated to the 9 classes grassland (managed), semi-natural habitats (mainly extensively grassland, fallow land and wetland), bushland (also including trees outside forest, hedges, scrups), water, settlements and four types of cropland (cereals, corn, rapeseed, other crops).

Following MCCOY (2005) and taking into account the resolution (5 m) of the satellite images and the positional accuracy of the remote sensing data and the field data, the minimum mapping unit (MMU) was determined with 500 m$^2$. In order to avoid mixed pixels and improve spectral separability, only the core areas of fields were analysed using a margin zone of 10 m for all objects. After applying the MMU and core area criteria and further taking into account the intersection of the coverage of the different satellite data sources, a total of 1581 patches remained for the analysis.

## 2.2 *Satellite Data*

In total, six RapidEye level 1B (RE1 – RE6), six TerraSAR-X stripmap (dual polarization) (TS1 – TS6) and four RADARSAT-2 scenes (fine beam Quad polarization) (RS1 and RS2) were successfully acquired during the growing season 2011. Fig. 1 shows extracts of colour composites for all satellite sensors together with an overview of the classification scheme. Fig. 2 illustrates the temporal distribution of the data acquisitions for all three sensors along the growing period from April to mid of August 2011. Due to weather constraints, no RapidEye acquisitions were possible after 29th June 2011. Heavy rainfall on 4th July also impacted the X-Band SAR image from TerraSAR-X and the acquisition could not be used for further investigations.

The processing of the RapidEye data included rigorous orthorectification after Toutin (2004), co-registration, atmospheric correction (ATCOR) and calculation of the normalized difference vegetation index (NDVI). All processing was done using PCI Geomatica 10.3 software (PCI 2013). The output is a dataset of six spectral parameters (blue, green, red, Red-Edge, NIR, NDVI) at 5 m spatial resolution for each acquisition. However, for analysis, only four parameters were used (green, Red-Edge, NIR, NDVI) to minimize redundancy in the input variables. RADARSAT-2 single look complex (SLC) data were filtered using the SCL Gaussian DE MAP Filter (Nezry & Yakam Simen 1999). Filtering was followed by a "Pauli coherent decomposition" of the fully polarimetric SLC dataset in terms of elementary scattering mechanisms (Cloude & Pottier 1996). Geometric and radiometric calibration (sigmaθ, dB) together with mosaicking of a pair of two adjacent scenes resulted in a dataset of six polarimetric layers (HH, HV, VV, Pauli1, Pauli2, Pauli3) at 5 m spatial resolution for each acquisition period (RS1 and RS2, Fig. 2).

TerraSAR-X SLC data were processed using a De Grandi multitemporal filter (deGrandi et al. 1997). Together with multilooking, coregistration and radiometric calibration, two filtered polarization layers (HH, HV) at 5 m

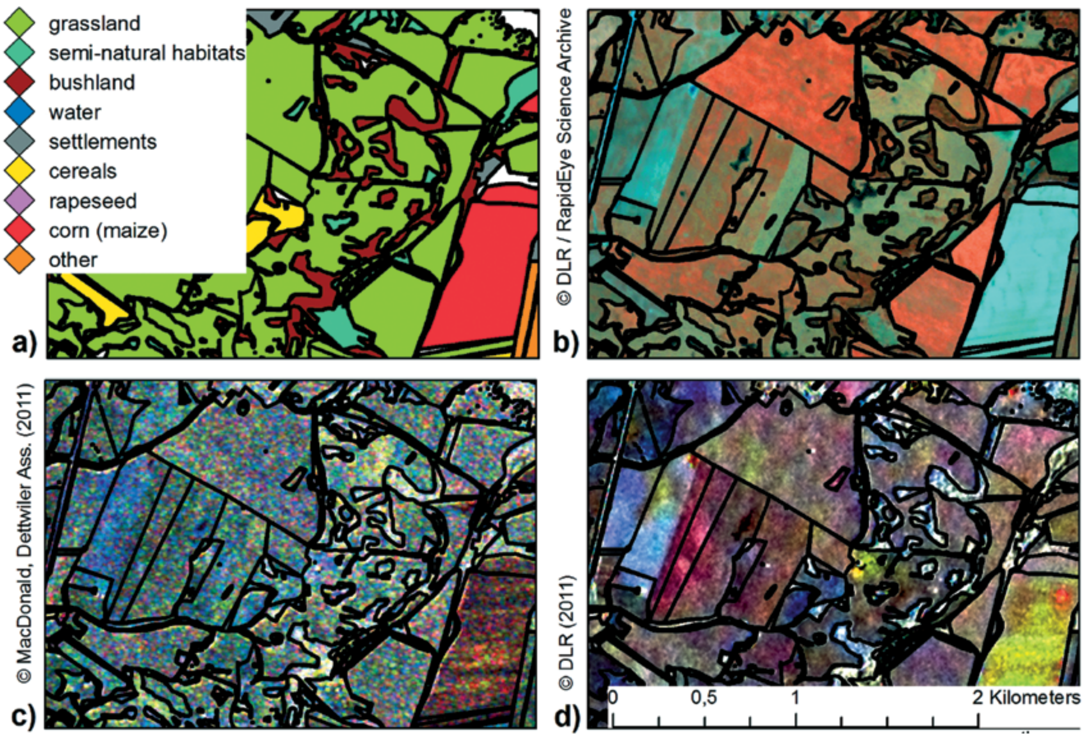


**Fig. 1:** Overview of data sources (a) ground truth, (b) RapidEye image (NIR, RE, G, 26th May 2011), (c) RADARSAT-2 image (VV,VH,HH; 20th May 2011), (d) TerraSAR-X image (17th August, 21st May, 7th April 2011).

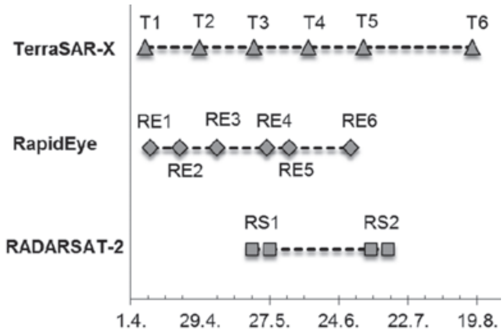


**Fig. 2:** Temporal profile of acquisitions for RapidEye and RADARSAT-2 and TerraSAR-X data.

spatial resolution were produced for each acquisition date. All SAR processing was done using ENVI/SarScape4.4 ® software.

## 3 Methods

### 3.1 *Image Classification*

The classification concept builds on the object (or patch) as the smallest entity. This means that each set of parameters from the optical and/or SAR data is examined at the patch-level of the existing ground truth base map. This ensures that every single object in the ground truth data base is assigned to a single land use type and within-field heterogeneity or mis-assignments are minimized. In the present study, spatial statistics (mean) were calculated at the patch level for each spectral and polarimetric parameter using standard GIS software (ESRI 2013). The outcome was a database of 46 independent variables that built the independent variables for the classifier. The variables were grouped by date of acquisition ($n = 13$) and by sensor ($n = 3$). In a first run, the information content of the variables was systematically evaluated using all possible combinations of acquisition dates for a single sensor system ($n = 89$). In the second run, only the best sensor-specific combinations of input variables were tested for synergy effects with the other two sensors systems. The precondition for the selection in the second run was based on the analysis of the quartiles of data distribution for all land cover types where only those classifications were chosen that are in the upper 10 %-quartile for at least two land cover categories. Out of this subset ($n = 16$), all possible bi-sensoral combinations ($n = 77$) between the three sensor systems were evaluated.

All classifications were run using a classification and regression tree (CART) algorithm (Breiman et al. 1984) in SPSS ® Version 20.0. Training data were selected from the ground truth dataset using a random split-sample validation approach with 30 % training and 70 % validation samples. Accuracy of the classification result was accounted for by calculating the overall accuracy assessment (OAA) as well as producer's accuracy (PA) and Cohen's kappa coefficient. Additionally, in order to evaluate the best predictors for every single classification, the normalized importance factor (*NI*) was computed (Erasmi et al. in press). The *NI* is based on the importance of each independent variable (input channel) for the regression tree classifier, weighted over the number of classification attempts where the variable was used:

$$NI_p = \sum_{i=1}^{n} \frac{I_{p,i}}{n} \tag{1}$$

where

$NI_p$ = normalized importance of independent variable $p$

$I_{p,i}$ = importance of parameter $p$ in classification $i$

$n$ = total number of classifications with parameter $p$

### 3.2 *Landscape Metrics*

Based on the classification results a number of selected landscape metrics were computed. The subset is oriented towards a comparison of different groups of metrics and their sensitivity to classification accuracy of the underlying land cover maps. The chosen subset includes area metrics (percentage of land cover type: PLAND), shape metrics (perimeter area ratio: PARA), diversity metrics (Shannon's diversity: SDI; Shannon's eveness: SEI; Dominance) as well as connectivity metrics (landscape division index: LDI). For a comparison and explanation of all metrics, see e.g. Riitters et al. (1995). Area, shape and connectivity metrics were calculated at the class level for four habitat types only. Diversity metrics can only be computed at the landscape level and made use of all available land cover types. All landscape metrics were calculated with V-LATE 2.0 beta for ArcGIS 10.0 (ZGIS 2013). Variability of landscape metrics values with regard to the entity of classification attempts was assessed by computing the normalized deviation of the landscape index values in relation to the metrics value of the reference data, $d_{p,i}$:

$$d_{p,i} = \frac{LI_{p,i}}{LI_{ref}} \tag{2}$$

where

$d_{p,i}$ = normalized deviation of landscape index $p$ for classification $i$

$LI_{p,i}$ = value of landscape index $p$ for classification result $i$

$LI_{ref}$ = landscape index value for reference classification

In order to avoid pseudo-variation in the landscape metrics due to inadequate input parameters (here: classification results), only classified images with an OAA of 75 % and higher were considered for landscape analysis. The similarity of the input data was further evaluated using a non-parametric hypothesis test for statistical dependence based on the tau coefficient (Kendall rank correlation). The output proved that, based on a significant difference at p = 0.01, all classified images were similar to the reference dataset ($n$ = 1580).

## 4 Results

### 4.1 *Classification and Accuracy Assessment*

Land cover classifications were run for all possible single-sensor combinations with regard to the date of acquisition. This yielded in a total of 57 classifications for RapidEye data (with one to six acquisition dates), 29 combinations for TerraSAR-X data (with on to five acquisitions) and three attempts for RADARSAT-2 data (single or bi-temporal acquisition). The OAA for all single-sensor combinations is given in Fig. 3. This graphical overview illustrates the considerable variability of OAA within a sensor-group and between sensor-systems. The CART-ID in Fig. 3 refers to a set of single-time to multi-temporal image combinations for the three sensor systems (see Fig. 2). The complexity of the input dataset for each sensor increases with the rank of the CART-ID. The results for RapidEye classifications show a general increase of OAA with increasing complexity of the input data (= number of acquisitions). However, highest OAA is achieved for a bi-temporal configuration using acquisitions RE3 and RE4 (beginning and end of May; CART-ID 15; OAA = 82.78 %). TerraSAR-X data perform significantly worse compared to RapidEye in terms of OAA. Best results were reached with a combination of four out of five acquisitions covering the whole investigation period from beginning of April until mid of August (CART-ID 82: T1,-2,-3,-5; OAA = 73.45 %). OAA values for RADARSAT-2 classifications are in the same magnitude as TerraSAR-X but with considerable lower OAA for the best classification result (mono-temporal, CART-ID 86: RS1; OAA = 66.83 %).

The second run of classifications aimed at the optimization of the previous results with regard to OAA and PA. This was accomplished using only selected bi-sensoral combinations of input datasets as described in the methods section. The graphical summary of

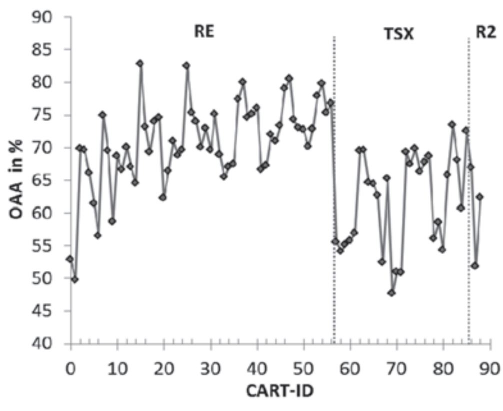


**Fig. 3:** Overall accuracy assessment (OAA) for single-sensor band combinations (RE = RapidEye, TSX = TerraSAR-X, R2 = RADARSAT-2).

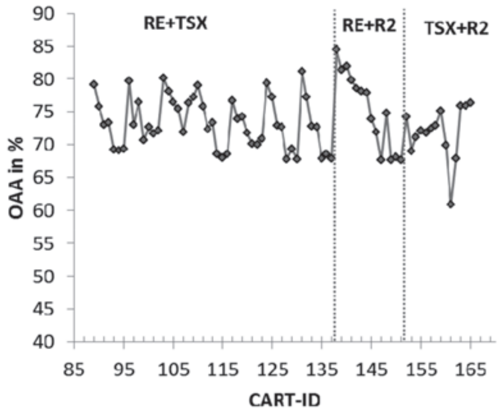


**Fig. 4:** Overall accuracy assessment (OAA) for bi-sensoral parameter combinations (RE = RapidEye, TSX = TerraSAR-X, R2 = RADARSAT-2).

OAA values for all 77 tested combinations is given in Fig. 4. Highest OAA for RapidEye and TerraSAR-X combinations is achieved for a combination of the best single-sensor datasets (CART-ID 131: RE3,-4,T1,-2,-3,-5; OAA = 81.13 %). However, the OAA is below the value for the RapidEye single-sensor classification. The variability of OAA for all RapidEye-/TerraSAR-X-attempts is lower compared to single-sensor classifications. RapidEye and RADARSAT-2 acquisitions yielded the highest OAA for all bi-temporal combinations. Again, the best result is achieved using the best single-sensor datasets (CART-ID 138: RE3,4,RS1; OAA = 84.53). In this case, the OAA increased more than 3 % compared to the highest single-sensor OAA. TerraSAR-X and RADARSAT-2 performed best for a combination of both RADARSAT-2 acquisitions together with the best single-sensor TerraSAR-X dataset (CART-ID 165: T1,-2,-3,-5, RS1,-2; OAA = 76.41 %).

The statistics of the producer's accuracy (PA) for all land cover types together with OAA for single-sensor and bi-sensoral classification configurations are summarized in Tab. 1. The variability of the PA is documented by the spread (minimum, maximum, coefficient of variation (*cv*)) and further characterized by the upper 10 %-quartile of the distribution function for the PA values. The lowest *cv* values for single-sensor observations are found for the class "grassland" (*cv* = 6.32 %). All other classes show considerably higher *cv* values even in cases where the 10 %-quartile is higher than 90 % (see classes "water", "bushland", "rapeseed", "corn" in Tab. 1). This is in accordance with the full data range of those classes and a minimum of 0 % for the classes "water", "rapeseed", "corn" and "other crops".

Bi-sensoral classification runs, in general, show lower variability with a *cv* for three classes below 10 % ("grassland", "bushland", "cereals"). Only two classes ("water", "other crops") could not be distinguished in at least one of the classification attempts. In both cases, "semi-natural habitats" perform under average. However, the variation of the accuracy significantly decreases with bi-sensoral approaches (21.68 % to 13.63 %). The comparison of the OAA statistics shows a substantial enhancement of the classification quality with a decrease of the *cv* from 11.93 % to 5.95 % and a remarkable increase in the mean OAA (67.46 % to 73.36 %) as well as the 10 %-quartile (76.15 % to 79.25 %).

Another focus within the systematic evaluation of the information content for the dataset of the three sensors was on the determination of the most relevant independent variables for mapping habitat type in the study area. The normalized importance factor (*NI*) provides an estimate of the importance of each independent variable (input channel) for the regression tree classifier. Fig. 5 presents a summary of the *NI* for 25 out of 46 variables. Highest *NI* is observed for input channel two (green light) of RapidEye acquisition no. six ($29^{th}$ June) followed by channel 4 (Red-Edge) of RE4 and RE3 ($26^{th}$ May and $06^{th}$ May). RADARSAT-2 variables are amongst the top ten highest NI values (mid of May, VV and HH polarized) and further spread throughout the whole chart. In contrast, TerraSAR-X variables are only present at the end of the list with two HH-polarized layers from end of April (T2) and mid of May (T3). The number of CART-runs (*n*) in Fig. 5 gives guidance towards the overall relevance of the variables with high *NI* values. The highest *n* values are connected to the RapidEye acquisitions RE3 and RE4. This is a consequence of the high PA and OAA values for RapidEye classifications including these two scenes. Hence, the maximum number of *n* = 63 CART-runs (RE/TS or RE/RS) is realized.

**Tab. 1:** Statistics of producer's accuracy (PA) for all land cover types and overall accuracy assessment (OAA) for single-sensor and bi-sensoral classification configurations.

| | Land cover type | Min | Max | Mean | Upper 10%-Quartile | Coefficient of Variation |
|---|---|---|---|---|---|---|
| PA single-sensor | Grassland | 64.72 | 95.75 | 83.89 | 89.04 | 6.32 |
| | Semi-natural habitats | 16.10 | 71.42 | 52.04 | 64.17 | 21.68 |
| | Water | 0.00 | 99.92 | 66.50 | 99.32 | 55.54 |
| | Bushland | 52.66 | 93.14 | 80.62 | 92.09 | 14.60 |
| | Settlements | 3.83 | 82.42 | 42.81 | 69.23 | 55.10 |
| | Cereals | 45.36 | 90.39 | 71.10 | 83.33 | 14.30 |
| | Rapeseed | 0.00 | 94.72 | 41.97 | 92.42 | 77.42 |
| | Corn (maize) | 0.00 | 95.01 | 65.53 | 90.44 | 37.67 |
| | Other crops | 0.00 | 64.62 | 21.53 | 55.75 | 92.17 |
| | Overall Accuracy | 47.69 | 82.78 | 67.46 | 76.15 | 11.93 |
| PA bi-sensoral | Grassland | 83.43 | 94.67 | 89.18 | 93.09 | 2.87 |
| | Semi-natural habitats | 34.29 | 71.84 | 58.71 | 66.18 | 13.63 |
| | Water | 0.00 | 99.57 | 63.07 | 99.52 | 53.63 |
| | Bushland | 71.32 | 93.99 | 87.45 | 92.55 | 6.50 |
| | Settlements | 14.41 | 71.04 | 62.94 | 70.36 | 20.22 |
| | Cereals | 71.52 | 92.58 | 80.55 | 87.00 | 5.91 |
| | Rapeseed | 5.65 | 93.94 | 34.53 | 78.70 | 71.34 |
| | Corn (maize) | 42.65 | 95.40 | 77.36 | 95.01 | 19.40 |
| | Other crops | 0.00 | 50.93 | 13.88 | 38.98 | 109.54 |
| | Overall Accuracy | 60.83 | 84.53 | 73.36 | 79.25 | 5.95 |

## 4.2 *Landscape Metrics and Uncertainty Assessment*

The land cover maps provided the base for the computation of landscape metrics at class and landscape level. As described earlier in the methods section, only classified images (single-sensor and bi-sensoral) with an OAA of at least 75 % were considered for analysis ($n = 42$).

The results of the landscape analysis for the study site are summarized in Tab. 2. The shape metrics at class level in general show low variation except for the class "rapeseed". Compared to this, the area metrics at class level indicate moderate to high variation with *cv* values ranging from 7.94 % to 24.46 %. Class connectivity metrics are in a close range around the reference map and landscape metrics show low to moderate variation in terms of the *cv*.

The main findings from the summary statistics are confirmed by a closer look at the data distribution for selected metrics at class and landscape level. In Fig. 6, the normalized deviation ($d_{p,i}$) is computed for "semi-natural habitat" class metrics (PARA, PLAND, LDI) compared to diversity metrics at landscape level. The graphs illustrate the high variation of area metrics (PLAND) compared to the connectivity and diversity metrics (SDI, SEI, Dominance).

The dissimilarity in sensitivity is mostly explained by the nature of the metrics itself. E.g., PLAND is directly and exclusively depending on changes in land cover composition that are caused by variations in classification results.

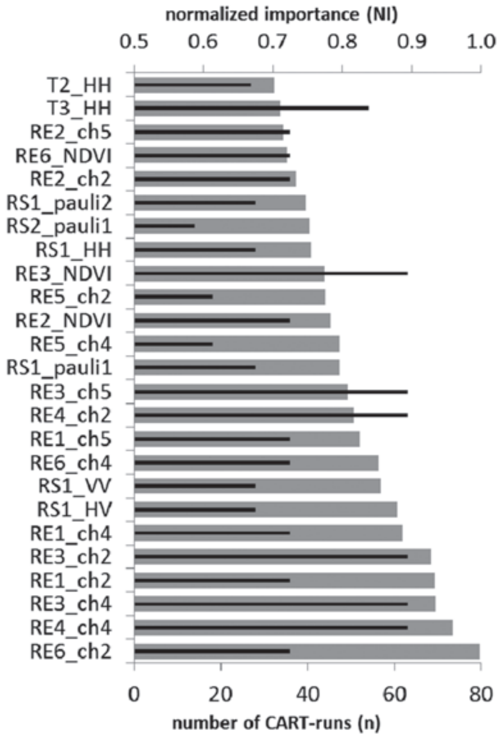


**Fig. 5:** Normalized importance factor (*NI*) of spectral and polarimetric parameters for all bi-sensoral classifications. A value of 1.0 means that the parameter shows highest relative importance (100 %) in all CART-runs (thin black lines = *n*, grey bars = *NI*).

On the other hand, diversity metrics like SDI are less sensitive to changes in landscape composition and configuration because they are focused on the occurrence of land cover types more than on the areal extent.

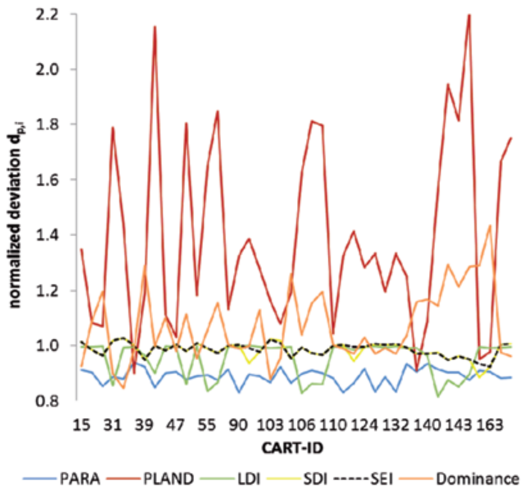


**Fig. 6:** Normalized deviation ($d_{p,i}$) of class metrics for semi-natural habitats and landscape metrics for all classifications with OAA higher 75 % ($n$ = 42) (PARA = perimeter area ratio, PLAND = percentage of land cover type, LDI = landscape division index, SDI = Shannon's diversity, SEI = Shannon's eveness).

**Tab. 2:** Statistics (normalized deviation, $d_{p,i}$) describing the variation of the landscape metrics at class and landscape level for selected habitat types in relation to ground truth data.

| Level | Group | Metric | Min | Max | Mean | Coefficient of variation |
|---|---|---|---|---|---|---|
| Class level | Shape | PARA_grassland | 1.06 | 1.23 | 1.15 | 3.10 |
| | | PARA_semi-natural | 0.83 | 0.94 | 0.89 | 3.13 |
| | | PARA_bushland | 0.91 | 1.02 | 0.98 | 2.54 |
| | | PARA_rapeseed | 0.77 | 2.66 | 1.19 | 46.33 |
| | Area | PLAND_grassland | 0.92 | 1.34 | 1.12 | 7.94 |
| | | PLAND_semi-natural | 0.90 | 2.21 | 1.39 | 24.46 |
| | | PLAND_bushland | 1.19 | 2.50 | 1.65 | 21.65 |
| | | PLAND_rapeseed | 0.43 | 1.07 | 0.93 | 12.88 |
| | Connectivity | LDI_grassland | 0.998 | 1.001 | 1.00 | 0.05 |
| | | LDI_semi-natural | 0.81 | 1.00 | 0.95 | 6.55 |
| | | LDI_bushland | 0.98 | 1.00 | 0.99 | 0.63 |
| | | LDI_rapeseed | 0.95 | 1.01 | 0.99 | 1.23 |
| Landscape level | Diversity | Shannon's Diversity | 0.89 | 1.03 | 0.98 | 2.97 |
| | | Shannon's Eveness | 0.92 | 1.03 | 0.99 | 2.44 |
| | | Dominance | 0.85 | 1.43 | 1.07 | 12.31 |

## 5 Discussion and Conclusions

The results of the land cover classifications confirm the general ability of optical high temporal and spatial resolution satellite data (RapidEye) for mapping and monitoring habitat types in a heterogeneous agricultural landscape. The accuracy of mapping considerably increases with the availability of multi-temporal datasets for the growing period. High accuracy could already be obtained with bi-temporal observations, where acquisitions at an early stage during the growing season yielded highest accuracy. The *NI*-index demonstrates the high impact of the spectral and temporal domain of the RapidEye time series. In particular, it stresses the relevance of the Red-Edge channel of the RapidEye system for mapping vegetated surfaces. Compared to this, the results of RADARSAT-2 and TerraSAR-X single-sensor classifications are significantly worse. Bi-sensoral combinations of optical and SAR-data yielded satisfying accuracy, where RADARSAT-2 polarimetric data outperform the TerraSAR-X time series with regard to its potential for synergistic optical/SAR habitat type mapping. However, the documented potential of optical-SAR fusion is clearly directed towards the availability of SAR data in mid-latitude regions with frequent weather constraints.

The landscape analysis in terms of class and landscape metrics shows diverse patterns of uncertainty that can be addressed by different groups of metrics. In general, the results show that area based metrics, e.g. percentage of land cover class, are most sensitive to classification accuracy and variability of mapping results. The magnitude of variation for those metrics is much higher than the classification errors. The same problem has been reported by Langford et al. (2006). Shape and connectivity measures at class level seem to be more resistant to changes in landscape composition and configuration. The same applies for diversity metrics at landscape level that are less affected by landscape composition which is in accordance with findings by Altamirano et al. (2012).

The results demonstrate that the choice of satellite sensor systems and acquisition periods essentially impact the result of habitat type mapping and hence directly influence any study that aims at quantifying the composition and configuration of landscapes for biological conservation issues. As shown here, variations in landscape metrics are the result of only slight changes in input variables for land cover classification approaches. The same problem arises, when different classification algorithms are used to map a landscape from identical input data as shown in Mas et al. (2010) or when spatial or thematic resolution is not a constant in the model (Baldwin et al. 2004, Buyantuyev & Wu 2007). On the other hand, there are groups of landscape metrics that are not affected by changes in landscape composition as reported also by Wickham et al. (1997). Therefore, comparison of landscape metrics for different regions or for temporal change analysis always has to account for the accuracy of the underlying land cover map and for the sensitivity of the landscape metrics to land cover variations.

## Acknowledgements

RapidEye data are provided by the RapidEye Science Archive (RESA) of the German Aerospace Center (DLR) within the project RESA-451. RADARSAT-2 data are provided by the Canadian Space Agency (CSA) and MacDonald, Dettwiler and Assoc. Ltd. under contract no. SOAR-5040. TerraSAR-X data are made available from DLR under contract no. LAN0901.

## References

Altamirano, A., Miranda, A. & Jimenez, C., 2012: Uncertainty of landscape indices for spatial structure analysis. – Bosque **33** (2): 171–181.

Baldwin, D.J., Weaver, K., Schnekenburger, F. & Perera, A.H., 2004: Sensitivity of landscape pattern indices to input data characteristics on real landscapes: implications for their use in natural disturbance emulation. – Landscape Ecology **19** (3): 255–271.

Breiman, L., Friedman, J.H., Olshen, R.A. & Stone, C.J., 1993: Classification and regression trees. – Chapman & Hall, New York, USA.

Buyantuyev, A. & Wu, J., 2007: Effects of thematic resolution on landscape pattern analysis. – Landscape Ecology **22** (1): 7–13.

Cloude, S.R. & Pottier, E., 1996: A review of target decomposition theorems in radar polarimetry. – IEEE Transactions on Geoscience and Remote Sensing **34** (2): 498–518.

Erasmi, S., Riembauer, G. & Westphal, C., in press: Mapping habitat diversity from multitemporal Rapid-Eye and RADARSAT-2 data in Brandenburg, Germany. – Borg, E. (ed.): Rapid-Eye Science Archive. – Gito, 20.–22. March 2013, Neustrelitz, Berlin.

ESRI, 2013: www.esri.com (19.2.2013).

Gillespie, T.W., Foody, G.M., Rocchini, D., Giorgi, A.P. & Saatchi, S., 2008: Measuring and modelling biodiversity from space. – Progress in Physical Geography **32** (2): 203–221.

de Grandi, G., Leysen, M., Lee, J. & Schuler, D., 1997: Radar reflectivity estimation using multiple SAR scenes of the same target: technique and applications. – Geoscience and Remote Sensing, 1997, IGARSS '97. Remote Sensing – A Scientific Vision for Sustainable Development. – 1997 IEEE International **2:** 1047–1050.

Langford, W.T., Gergel, S.E., Dietterich, T.G. & Cohen, W., 2006: Map misclassification can cause large errors in landscape pattern indices: Examples from habitat fragmentation. – Ecosystems **9** (3): 474–488.

Lechner, A.M., Langford, W.T., Bekessy, S.A. & Jones, S.D., 2012: Are landscape ecologists addressing uncertainty in their remote sensing data? – Landscape Ecology **27** (9): 1249–1261.

Mas, J.-F., Gao, Y. & Navarrete Pacheco, J.A., 2010: Sensitivity of landscape pattern metrics to classification approaches. – Forest Ecology and Management **259** (7): 1215–1224.

McCoy, R.M., 2005: Field methods in remote sensing. – Guilford Press, New York.

Neel, M.C., McGarigal, K. & Cushman, S.A., 2004: Behavior of class-level landscape metrics across gradients of class aggregation and area. – Landscape Ecology **19** (4): 435–455.

Nezry, E. & Yakam Simen, F., 1999: A family of distribution-entropy MAP speckle filters for polarimetric SAR data, and for single or multichannel detected and complex SAR images. – CEOS SAR Workshop (ESA SP-450): 219–223.

PCI, 2013: PCI Geomatics Incorporated. – www.pcigeomatics.com (19.2.2013).

Perovic, D.J., Gurr, G.M., Raman, A. & Nicol, H.I., 2010: Effect of landscape composition and arrangement on biological control agents in a simplified agricultural system: A cost-distance approach. – Biological Control **52** (3): 263–270.

Riitters, K.H., O'Neill, R.V., Hunsaker, C.T., Wickham, J.D., Yankee, D.H., Timmins, S.P., Jones, K.B. & Jackson, B.L., 1995: A factor analysis of landscape pattern and structure metrics. – Landscape Ecology **10** (1): 23–39.

Saura, S., 2002: Effects of minimum mapping unit on land cover data spatial configuration and composition. – International Journal of Remote Sensing **23** (22): 4853–4880.

Toutin, T., 2004: Review article: Geometric processing of remote sensing images: models, algorithms and methods. – International Journal of Remote Sensing **25** (10): 1893–1924.

Tscharntke, T., Tylianakis, J.M., Rand, T.A., Didham, R.K., Fahrig, L., Batáry, P., Bengtsson, J., Clough, Y., Christ, T.O., Dormann, C.F., Ewers, R.M., Fründ, J., Holt, R.D., Holzschuh, A., Klein, A.M., Kleijn, D., Kremen, C., Landis, D.A., Laurance, W., Lindenmayer, D., Scherber, C., Sodhi, N., Steffan-Dewenter, I., Thies, C., van der Putten, W.H. & Westphal, C., 2012: Landscape moderation of biodiversity patterns and processes – eight hypotheses. – Biological Reviews **87** (3): 661–685.

Westphal, C., Steffan-Dewenter, I. & Tscharntke, T., 2006: Bumblebees experience landscapes at different spatial scales: possible implications for coexistence. – Oecologia **149** (2): 289–300.

Wickham, J.D., ONeill, R.V., Riitters, K.H., Wade, T.G. & Jones, K.B., 1997: Sensitivity of selected landscape pattern metrics to land-cover misclassification and differences in land-cover composition. – Photogrammetric Engineering and Remote Sensing **63** (4): 397–402.

ZGIS, 2013: Universität Salzburg, Department of Geoinformatics. – www.zgis.at (19.2.2013).

Address of the Author:

Dr. Stefan Erasmi, Cartography, GIS & Remote Sensing Department, Institute of Geography, Georg-August-University Göttingen, Goldschmidtstraße 5, D-37077 Göttingen, Germany, e-mail: serasmi@uni-goettingen.de

Manuskript eingereicht: November 2012
Angenommen: Februar 2013